Dipole Blockade at Förster Resonances in High Resolution Laser Excitation of Rydberg States of Cesium Atoms

Thibault Vogt,* Matthieu Viteau, Jianming Zhao,† Amodsen Chotia, Daniel Comparat, and Pierre Pillet
Laboratoire Aimé Cotton, CNRS, Bâtiment 505, Campus d'Orsay, 91405 Orsay, France
(Received 5 March 2006; published 24 August 2006)

High resolution laser excitation of np Rydberg states of cesium atoms shows a dipole blockade at Förster resonances corresponding to the resonant dipole-dipole energy transfer of the $np + np \rightarrow ns + (n+1)s$ reaction. The dipole-dipole interaction can be tuned on and off by the Stark effect, and such a process, observed for relatively low $n(25–41)$, is promising for quantum gate devices. Both Penning ionization and saturation in the laser excitation can limit the range of observation of the dipole blockade.

DOI: 10.1103/PhysRevLett.97.083003 PACS numbers: 32.80.Rm, 32.80.Pj, 34.20.Cf, 34.60.+z

Rydberg atoms have long been known to have huge polarizabilities leading to exaggerated collisional properties of room temperature atoms, in particular, large cross sections and long interaction times [1]. These properties have stimulated great interest in the possibility of controlling the strong long-range interactions between cold atoms [2–4], which could be particularly exciting for quantum information applications [5,6]. One interesting process is the possibility of the dipole blockade in the Rydberg excitation of atoms, due to the dipole-dipole interaction shifting the Rydberg energy from its isolated atomic value. The use of the dipole blockade of the excitation has been proposed as a very efficient realization of a scalable quantum logic gate [6]. In a large ensemble of atoms, the first excited Rydberg atoms shift the resonance for their nonexcited neighbors and prevent their excitation with a narrow-bandwidth laser. A partial, or local, blockade of the Ryderg excitation is expected. If the volume of the laser excitation is small enough, no two-atom collective excitation can occur, producing an atomic ensemble in a singly excited collective state.

Up until now, there has been no evidence of a dipole blockade. In a zero electric field, atomic Rydberg states do not have permanent dipole moments, and no dipole blockade is expected. Second order dipole-dipole or van der Waals coupling between Rydberg atoms can occur, and a suppression of the excitation corresponding to a partial, or local, blockade has been reported in excitation of high Rydberg states ($n \sim 70–80$) using a pulsed amplified single mode laser [7]. Cw excitations have also been performed showing the suppression of the excitation [8] and studying the sub-Poissonian atom counting statistics [9]. It has been noticed that, for long-duration excitations, the appearance of ions can prevent the observation of the blockade [9]. Another limitation of the blockade which we underscore in this Letter is laser power broadening. For a broadband excitation, the suppression of the excitation is not expected. Rather a band of levels can be excited with a density-dependent broadening, which has been probed using microwave transitions [10,11], or laser depumping [12]. In the presence of an electric field, Rydberg atoms can have a significant permanent dipole moment, but different couplings should be considered to understand the behavior of the excitation and of the blockade. A simpler situation is to use a configuration similar to Förster resonances [13] which corresponds to a strong and dominant dipole-dipole coupling at low electric field. The Förster (or fluorescence) resonance energy transfer is commonly used as a spectroscopic technique based on long-range dipole-dipole coupling to estimate small distances and dynamics between fluorescent molecules [14,15].

In this Letter, we report the observation of the dipole blockade of the cesium Rydberg excitation using cw lasers. We take advantage of the Förster resonance (FR)

$$np_{3/2} + np_{3/2} \rightarrow ns + (n+1)s, \qquad (1)$$

obtained when the $np_{3/2}$ Stark level is Stark shifted midway in the energy diagram between the levels ns and $(n+1)s$ [2], which exists only for $n \leq 41$. The average dipole-dipole interaction is given by $W \sim \mu\mu' R^{-3}$, where $\mu, \mu' \sim n^2$ a.u. are the dipoles corresponding to the transitions $np_{3/2} \rightarrow ns$ and $np_{3/2} \rightarrow (n+1)s$, respectively, and R is the interatomic distance. At FR, we observe a significant decrease $\sim 30\%$ of the total number of excited (s and p) Rydberg atoms N_{tot} interpreted as the result of a dipole blockade.

The details of the experimental setup have been described in several papers [2,4,12]. Here three cw lasers provide a high resolution multistep scheme of excitation, as depicted in Fig. 1(a). The Rydberg atoms are excited from a cloud of 5×10^7 cesium atoms (temperature 200 μK, characteristic radius ~ 300 μm, peak density 1.2×10^{11} cm^{-3}) produced in a standard vapor-loaded magneto-optical trap (MOT). The first step of the excitation, $6s$, $F = 4 \rightarrow 6p_{3/2}$, $F = 5$, is provided by the trapping lasers (wavelength $\lambda_1 = 852$ nm). The density of excited, $6p_{3/2}$, atoms can be modified by switching off the repumper lasers before the excitation sequence. The second step, $6p_{3/2}$, $F = 5 \rightarrow 7sF = 4$, is provided by an infrared diode laser in an extended cavity device (wavelength $\lambda_2 = 1.47$ μm, bandwidth 100 kHz, and available

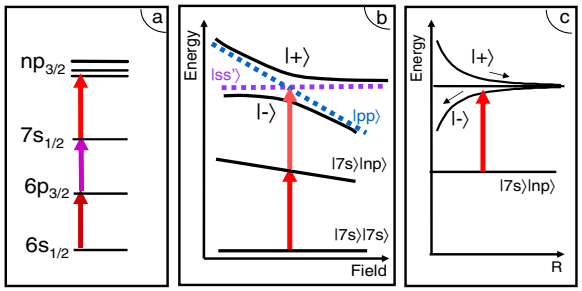

FIG. 1 (color online). (a) Three-step scheme of excitation for $np_{3/2}$ Rydberg levels. (b) Excitation of a pair of atoms at the Förster resonance. The dipole-dipole coupling $W \sim \mu\mu' R^{-3}$ leads to an avoided crossing between the energy levels of the pair of atoms $pp \equiv |np_{3/2}\rangle \otimes |np_{3/2}\rangle$ and $ss' \equiv |ns\rangle \otimes |(n+1)s\rangle$. At resonance, the eigenstates are $|+\rangle = (pp + ss')/\sqrt{2}$ and $|-\rangle = (pp - ss')/\sqrt{2}$. (c) Internuclear energy dependence and excitation of the states $|+\rangle$ and $|-\rangle$ states corresponding to mutual repulsive and attractive forces between the two atoms, respectively.

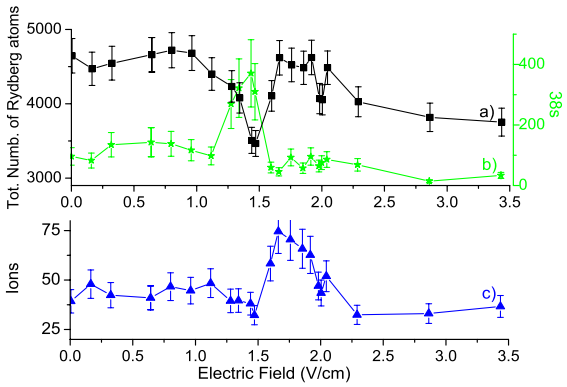

FIG. 2 (color online). Dipole blockade for the $38p_{3/2}$ level versus the applied electric field for a $7s$-atom density $\sim 8 \pm 3 \times 10^9$ cm^{-3}. For each recorded point of the curves, the Ti:Sa laser is resonant with the transition $7s \rightarrow 38p_{3/2}$, with a power ~ 8 mW corresponding to an average intensity of 45 W/cm^2. (a) Total number of Rydberg atoms, (b) number of $38s$ atoms, and (c) number of ions. (a)–(c) Error bars indicate measurement uncertainties.

power 20 mW). The experimental average intensity is ~ 3 mW/cm^2, twice the saturation one. The last step of the excitation, $7s$, $F = 4 \rightarrow np_{3/2}$ (with $n = 25$–45), is provided by a titanium:sapphire (Ti:Sa) laser. The wavelength λ_3 ranges from 770 to 800 nm, the bandwidth is 1 MHz, and the available power is 400 mW. The Ti:Sa laser is switched on during a time $\tau = 0.3$ μs by means of an acousto-optic modulator. The beams of the infrared diode laser and Ti:Sa laser cross with an angle of 67.5° and are focused into the atomic cloud with waists of 105 and 75 μm, respectively. Their polarizations are both linear and parallel to the direction of the applied electric field, leading to the excitation of the magnetic sublevel $np_{3/2}$ $|m| = 1/2$. The spectral resolution $\Delta\nu_L$ of the excitation is of the order of 6 MHz, limited by the lifetime 56.5 ns of the $7s$ state and by the duration and the spectral width of the Ti:Sa laser pulse. The magnetic quadrupole field of the MOT is not switched off during the Rydberg excitation phase; it contributes less than 1 MHz to the observed linewidths. The Rydberg atoms are selectively ionized and then detected by applying, just after the Ti:Sa laser pulse, a high field pulse with a rise time of 700 ns.

The experimental procedure is based on spectroscopy of Stark $np_{3/2}$ states by scanning the optical frequency of the Ti:Sa laser pulse at a repetition rate of 80 Hz for different atomic densities and for different Ti:Sa laser intensities.

Figure 2(a) shows the field dependence of the total number of Rydberg atoms N_{tot} when the Ti:Sa laser is resonant with the transition $7s \rightarrow 38p_{3/2}$. At zero field, N_{tot} is about 4700, which gives an estimation of the peak density 3.0×10^9 cm^{-3}. The figure exhibits a marked minimum of N_{tot} at FR (reaction 1) for $F = 1.46$ V/cm. Such a result is interpreted as the signature of the dipole blockade. It means that no pairs of close atoms can be excited at FR if the dipole-dipole coupling W exceeds the resolution of the laser excitation $\Delta\nu_L \sim 6$ MHz, i.e., if the interatomic spacing $R \sim (\mu\mu'/W)^{1/3}$ is smaller than $R_{\text{min}} \sim (\mu\mu'/\Delta\nu_L)^{1/3}$. For $n = 38$, we obtain $R_{\text{min}} \sim 4$ μm, which is compatible with the average interatomic distance in the center of the Rydberg cloud $R_{\text{av}} \sim 4.8$ μm deduced from the measured Rydberg atom number and peak density 3400 and 2.2×10^9 cm^{-3}, respectively (the corresponding mean dipole-dipole interation is $W_{\text{av}} \sim 3.3$ MHz). Outside FR, N_{tot} is relatively constant at low fields but decreases at fields higher than 2.5 V/cm. As mentioned in the introduction, the $p, d, \ldots$ characters in the Stark p level create a permanent atomic dipole and modify the excitation and interatomic couplings. Studies on these couplings are in progress and are not the subject of this Letter. Figure 2(b) shows the field evolution of the population transferred in the $38s$ level, selectively detected. The s transfer signal is maximum at FR with the same FR field width (FWHM) as the one observed in Fig. 2(a) for N_{tot}. Figure 2(c) corresponds to a weak ion signal which is recorded with the Rydberg one. Their number is less than 1% of N_{tot}, relatively constant except on the high field wing of FR, where the number of ions increases up to $\sim$2%. As shown in Fig. 1(c), on the high field wing of FR, pairs of close atoms are excited in a situation of a mutual attractive dipolar force [4,12], responsible for Penning ionization [16]. This weak number of ions adds no broadening to the Rydberg resonance lines. Similar features to those of Fig. 2 are obtained for FRs with $n = 25$–41. For $n \geq 42$, the FR no longer exists. A limitation of the excitation at zero field is, nevertheless, observed for $n = 42$ because the small energy gap -9.5 MHz between pp and ss' pairs corresponds to a quasi-Förster resonance.

The effect of the dipole blockade depends on the initial atomic density (here the $7s$ density), as it is analyzed for the $36p_{3/2}$ FR which occurs at $F = 2.52$ V/cm [Fig. 3(a)]. Figure 3(b) displays two spectra of the resonance line, one recorded far from FR at $F' = 0.86$ V/cm (labeled 1), the other one at FR (labeled 2). At FR, a clear effect of the dipole blockade appears in the center of the line with a 30% dipole blockade of the excitation. The dipole blockade does not occur in the wings of the resonance lines mostly due to the reduced number of excited Rydberg atoms. Figure 3(c) compares the total number of Rydberg atoms excited at FR versus the one outside FR (at 1.37 V/cm) for two different peak densities of $7s$ atoms, $D \sim 8 \pm 3 \times 10^9$ cm^{-3} (case also considered in Figs. 2 and 4) and $D/3 \sim 2.7 \times 10^9$ cm^{-3}. For each density, the number of Rydberg atoms is increased by raising the Ti:Sa laser power. The effect of the dipole blockade is characterized by the gap between the experimental data and the straight line of slope 1. In both cases, it appears when more than 1000 Rydberg atoms are excited [see the solid line arrows in Fig. 3(c)] and both curves present the same evolution up to 2000 Rydberg excited atoms at FR. Then the evolutions differ, the dipole blockade being much less efficient for the density $D/3$. This behavior is due to the laser power saturation of the excitation ($\propto n^3$), reached when the Rabi frequency associated with the $7s \rightarrow np_{3/2}$ transition is close to the spontaneous emission rate of the $7s$ level. For both densities, the maximum blockade is reached at a $\sim$8 mW laser power [see the two dashed arrows in Fig. 3(c)] and becomes less efficient for a higher power. Figure 3(d) shows outside FR the appearance of the broadening of the Rydberg resonance lines with the laser power. The resolution of the laser excitation $\Delta\nu_L$ increases from 6 to 12 MHz. Thus, the excitation of pairs of closer atoms becomes possible at FR, preventing the dipole blockade. As mentioned before, at FR the dipole blockade is more efficient in the center of the line than on the wings, leading to an apparent broadening compared to the linewidths far from FR [see Figs. 3(b) and 3(d)]. To conclude, three kinds of conditions have to be fulfilled to realize the dipole blockade: the control of spurious effects (ions or stray fields), the nonsaturated laser excitation, and the highest possible spectral resolution. The measured dipole blockade rates depend on our experimental conditions and could be optimized especially at low $n \sim 25$, where they are strongly limited by the power saturation reached at $\sim$2.5 mW. The dependence of the dipole-dipole interaction with the angular distribution of atoms [17] will provide the ultimate limit for the efficiency of the dipole blockade.

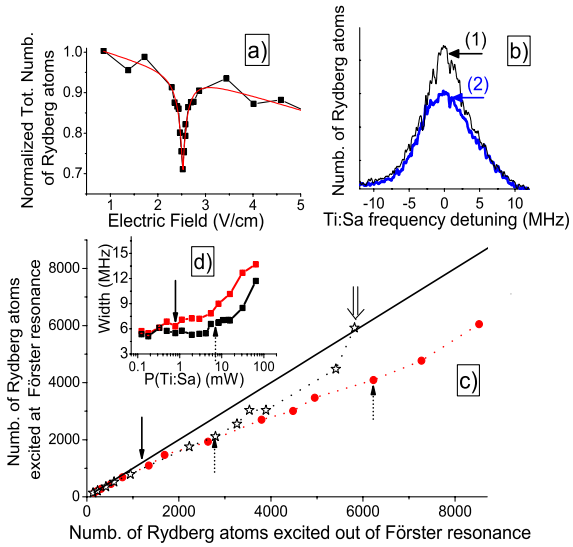

FIG. 3 (color online). Dipole blockade for the $36p_{3/2}$ level. Similar conditions as Fig. 2 are used in (a) and (b). (a) Field sweep of the FR. The signal is normalized to one at 0.86 V/cm. (b) Excitation spectral lines for two different fields: (1) at FR ($F = 2.52$ V/cm) and (2) off FR at 0.86 V/cm. (c) Total number of Rydberg atoms at FR versus the one off FR ($F' = 1.37$ V/cm), for the $7s$-atom densities $D \sim 8 \pm 3 \times 10^9$ cm^{-3} (solid circles) and $D/3$ (empty stars). The Ti:Sa power ranges 0–14 and 0–67 mW for the D and $D/3$ densities, respectively. (d) Linewidths of the $7s \rightarrow 36p_{3/2}$ spectral line, versus the Ti:Sa power P at both fields F (upper curve) and F' (lower curve). (c) and (d) Solid line arrows indicate the beginning of the dipole blockade, dashed arrows the beginning of the line broadening due to the power saturation. (c) A double down arrow indicates the complete power saturation of the excitation [P(Ti:Sa) > 60 mW] in the case of the $D/3$ density (the blockade is no longer observed). A similar result is obtained for the D density when the number of Rydberg atoms reaches $\sim$12 000.

After conversion of the $38p_{3/2}$ and $38s$ FR widths [shown in Fig. 2(a)] to frequency by using the Stark shift of the p level [see Fig. 1(b)], we obtain 50 ± 10 MHz

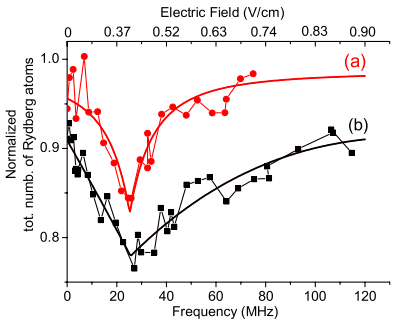

FIG. 4 (color online). Normalized total number of excited $41p_{3/2}$ Rydberg atoms versus the Stark shift (V/cm and MHz) of the $41p_{3/2}$ Stark level. The electric field has been converted to frequency using the experimental Stark shifts, in agreement with calculated ones. The two curves correspond to two different Rydberg atom number at Förster resonance, 3000 (circles) and 5000 (squares), obtained for laser powers 8 and 20 mW, respectively. The normalization factor is the number of atoms excited at a higher frequency (200 MHz). The fits use an empirical law not given here. The widths (FWHM) of the above Förster resonances are 20 ± 5 and 90 ± 30 MHz, respectively.

(FWHM). In this experiment, the FR width is 1 order of magnitude larger than the mean dipole-dipole interaction W_{av}, limited by the resolution of excitation $\Delta\nu_L$. This result appears surprising but is in agreement with the measured FR widths of the s transfer in the experiments with a broadband laser excitation [2,3,12]. The interpretation of those experiments is based on the interplay between two-body and many-body effects [11,18,19]. The latter includes the migration of the s excitation [ns or $(n+1)s$] in the p state environment by excitation exchange due to dipole-dipole resonant exchange processes

$$ns + np_{3/2} \rightarrow np_{3/2} + ns$$
$$\text{and} \quad (n+1)s + np_{3/2} \rightarrow np_{3/2} + (n+1)s. \tag{2}$$

The many-body effects have been experimentally investigated in detail [11] by modifying the Rydberg environment. They are roughly analogous to the diffusion of spins in glass. The role of reactions (2) probably has to be considered in our experiment. Figure 4 shows the FR plotted versus the Stark frequency shift in the case of the $41p_{3/2}$ level for two different numbers of Rydberg atoms at FR, 3000 (curve a) and 5000 (curve b). The dipole blockade leads, respectively, to $\sim$15% and 25% suppression of the Rydberg excitation and the FR widths are 20 and 90 MHz, respectively. FR (a) presents a symmetric resonance shape, while FR (b) is asymmetric, indicating a different dynamics for pairs of excited atoms submitted to a mutual repulsive (weak electric field) or attractive (strong electric field) force [see Fig. 1(c)]. The full analysis will require consideration of the dynamics of the interacting atoms, the saturation of the excitation, and many-body effects occurring during the excitation.

To conclude, we have observed evidence of a 30% dipole blockade of the Rydberg excitation at Förster resonance, controlled via the Stark effect. The observation of the total dipole blockade, meaning a single atom collective excitation, is still a challenge. It implies a volume of the Rydberg sample with a radius of the order of R_{min}. Here we observe the Förster resonance up to $n = 41$, limiting R_{min} at the value of 4 μm. The choice of another Förster configuration with n of the order of 100 or more increases R_{min} up to 20 μm. This result is promising for future developments in quantum information. A microwave field instead of a static electric field can also be used to produce the dipole moments and to control the dipole blockade [20]. Understanding and controlling the dipole-dipole interaction are important to prevent the formation of ions in a cold Rydberg sample and to induce its evolution towards an ultracold correlated plasma [21,22]. The band of levels due to the Rydberg interactions can be probed by laser or microwave excitation, to test the decoherence in such quantum complex systems [10–12]. The shape of the resonances can also be an excellent probe to test, for instance, the random character of the distribution of the pairs of atoms [23].

This work is in the frame of "Institut francilien de recherche sur les atomes froids" (IFRAF) and of the European Research and Training Networks COLMOL (No. HPRN-CT-2002-00290) and QUACS (No. HPRN-CT-2002-00309). One of the authors (J. Z.) is supported by IFRAF. The cw excitation development corresponds to a preliminary study for the CORYMOL experiment supported by an ANR grant (No. NT05-2 41884). The authors thank D. A. Tate for his helpful participation in preliminary work on this experiment and acknowledge very fruitful discussions with Thomas F. Gallagher, Marcel Mudrich, Nassim Zahzam, Paul Berman, and Vladimir Akulin. Laboratoire Aimé Cotton is associated to Université Paris-Sud and belongs to Fédération de Recherche Lumière Matière (LUMAT).

*Electronic address: thibault.vogt@lac.u-psud.fr
†Visiting scientist from College of Physics and Electronics Engineering, Shanxi University, China.

[1] T. F. Gallagher, *Rydberg Atoms* (Cambridge University Press, Cambridge, England, 1994).
[2] I. Mourachko *et al.*, Phys. Rev. Lett. **80**, 253 (1998).
[3] W. R. Anderson *et al.*, Phys. Rev. Lett. **80**, 249 (1998).
[4] A. Fioretti *et al.*, Phys. Rev. Lett. **82**, 1839 (1999).
[5] D. Jaksch *et al.*, Phys. Rev. Lett. **85**, 2208 (2000).
[6] M. D. Lukin *et al.*, Phys. Rev. Lett. **87**, 037901 (2001).
[7] D. Tong *et al.*, Phys. Rev. Lett. **93**, 063001 (2004).
[8] K. Singer *et al.*, Phys. Rev. Lett. **93**, 163001 (2004).
[9] T. CubelLiebisch *et al.*, Phys. Rev. Lett. **95**, 253002 (2005).
[10] K. Afrousheh *et al.*, Phys. Rev. Lett. **93**, 233001 (2004).
[11] I. Mourachko *et al.*, Phys. Rev. A **70**, 031401(R) (2004).
[12] M. Mudrich *et al.*, Phys. Rev. Lett. **95**, 233002 (2005).
[13] T. F. Gallagher *et al.*, Phys. Rev. A **25**, 1905 (1982).
[14] T. Förster, *Modern Quantum Chemistry* (Academic, New York, 1996).
[15] T. Förster, Discuss. Faraday Soc. **27**, 7 (1959).
[16] W. Li *et al.*, Phys. Rev. Lett. **94**, 173001 (2005).
[17] T. G. Walker and M. Saffman, J. Phys. B **38**, S309 (2005).
[18] W. M. Akulin *et al.*, Physica (Amsterdam) **131D**, 125 (1999).
[19] J. S. Frasier *et al.*, Phys. Rev. A **59**, 4358 (1999).
[20] P. Pillet *et al.*, Phys. Rev. A **36**, 1132 (1987).
[21] M. P. Robinson *et al.*, Phys. Rev. Lett. **85**, 4466 (2000).
[22] W. Li *et al.*, Phys. Rev. A **70**, 042713 (2004).
[23] V. M. Akulin, *Coherent Dynamics of Complex Quantum Systems* (Springer, New York, 2006).